Supporting Information

Activating rhodium phosphide-based catalysts for pH-universal hydrogen evolution reaction

Zonghua Pu,[a] Ibrahim Saana Amiinu,[a] Daping He,[a,b] Min Wang,[a] Guoqiang Li[c]*,and Shichun Mu[a*]

[a] State Key Laboratory of Advanced Technology for Materials Synthesis and Processing, Wuhan University of Technology, Wuhan 430070, P. R. China.

[b] Hubei Engineering Research Center of RF-Microwave Technology and Application, Wuhan University of Technology, Wuhan 430070, P. R. China.

[c] Department of Electronic Materials, South China University of Technology, Guangzhou 510641, P. R. China

* E-mail: msc@whut.edu.cn, msgli@scut.edu.cn

1. **Experimental Section**

Materials: $RhCl_3 \cdot xH_2O$ and melamine were purchased from Xinglong Chemical Corp. Ltd. H_2SO_4 and KOH were purchased from Beijing Chemical Works Ltd. $NH_4H_2PO_4$, K_2HPO_4, KH_2PO_4, and ethanol were purchased from Aladdin Reagents Ltd. Myoinositol 1,2,3,4,5,6-hexakisphosphate (MH), Pt/C (20 wt%) and Nafion (5 wt%) were purchased from Sigma-Aldrich. All chemicals are analytical grade and used as received without further purification. High-purity water was supplied by a Millipore system.

Preparation of Rh_2P@NC: $RhCl_3 \cdot xH_2O$ and MH and were dissolved in water by stirring, followed by addition of melamine. Then, the solution was dried at 60 ℃ 12 h to form a homogeneous powder. The solid mixture was then annealed at 900 °C for 120 min under nitrogen atmosphere with a heating rate of 5 ℃ min^{-1}. After cooled to room temperature, the black product was collected, washed by centrifugation with alcohol and water several times to remove the residue of reactants, and finally dried under oven at 80 °C overnight. A black powder material of Rh_2P@NC was obtained. For comparision, the Rh/NC was also made via the same steps as Rh_2P@NC without adding MH.

Preparation the working electrode: 10.0 mg of the catalyst powder was dispersed in 990 μL water/ethanol (v/v=1:1) mixed solvents along with 10 μL 5 wt% of Nafion solution, and the mixed solution was sonicated for 10 min. Then 5 μL of the catalyst ink was loaded on a glassy carbon electrode (GCE: diameter = 3 mm).

Electrochemical measurements: The HER electrochemical measurements are performed in a standard three-electrode with two-compartment cell on an electrochemical workstation (CHI 660E). The acidic (0.5 M H_2SO_4), neutral (1.0 M PBS) and alkaline (1.0 M KOH) electrochemical measurements were performed using a saturated calomel electrode (SCE) as the reference electrode. A graphite plate was used as the counter electrode in all measurements. Polarization data were obtained at a scan rate of 5 mV s^{-1}. In all measurements, the reference electrode was calibrated with respect to reversible hydrogen electrode (RHE). The calibration was performed in the high purity hydrogen saturated electrolyte with a Pt wire as the working electrode. The current-voltage was run at a scan rate of 2 mV s^{-1}, and the average of the two potentials at which the current crossed zero was taken to be the thermodynamic potential for the hydrogen electrode reactions. All polarization curves were iR-corrected. Electrochemical impedance spectroscopy (EIS) measurements were carried out in the frequency range of 100 kHz–0.1 Hz with an AC amplitude of 10 mV. iR compensation was applied for all the electrochemical measurements. The Faradic efficiency (FE) is defined as the ratio of the amount of experimentally determined hydrogen to that of the theoretically expected hydrogen. The hydrogen gas was collected by the water drainage method. A constant potential was applied on the electrode and the volume of evolved gases was recorded synchronously. Then the moles of H_2 were calculated based on the gas laws. The theoretically expected amount of H_2 was then calculated by applying the Faraday law, which states that the passage of 96500 C causes 1 equivalent of reaction.

Characterization: Powder X-ray diffraction (XRD) patterns were collected on a Rigaku X-ray diffractometer equipped with a Cu Kα radiation source. XPS measurements were performed on an ESCALABMK II X-ray photoelectron spectrometer using Mg as the exciting source. SEM measurements were carried out on a XL30 ESEM FEG scanning electron microscope at an accelerating voltage of 20 kV. TEM measurements were performed on a HITACHI H-8100 electron microscopy (Hitachi, Tokyo, Japan) with an accelerating voltage of 200 kV. Raman spectra were obtained on J-Y T64000 Raman spectrometer with 514.5 nm wavelength incident laser light.

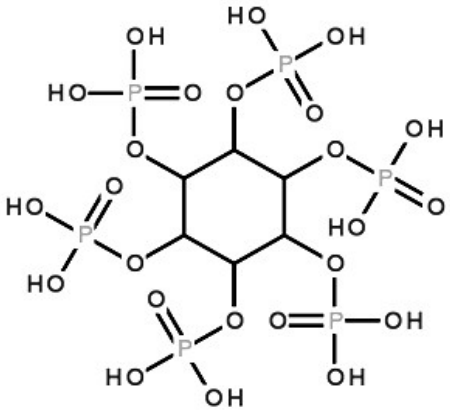

Fig. S1 Molecular structure of MH.

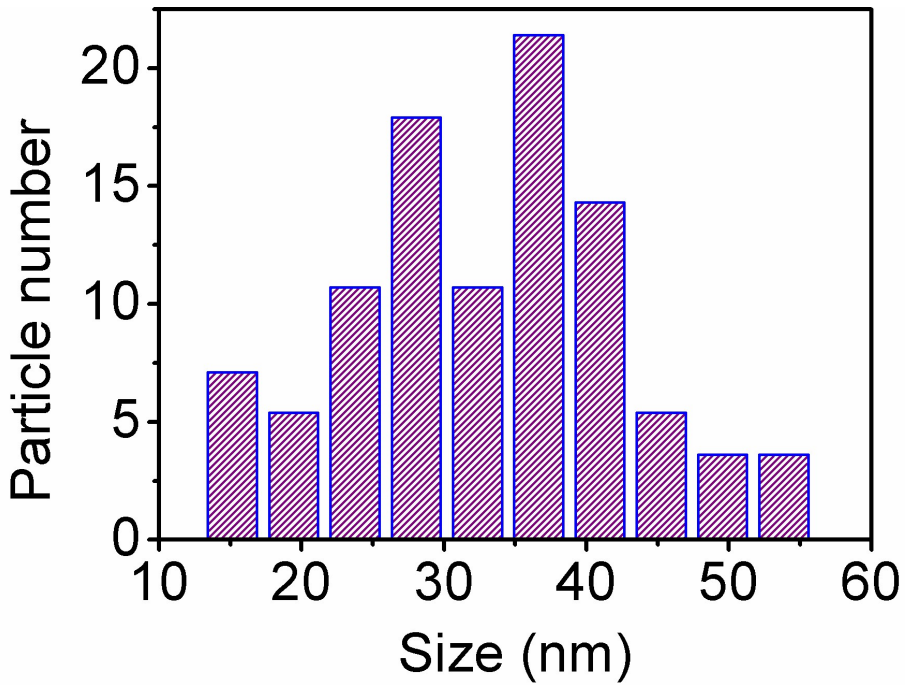

Fig. S2 Size distribution of Rh_2P nanoparticles in Rh_2P@NC**.**

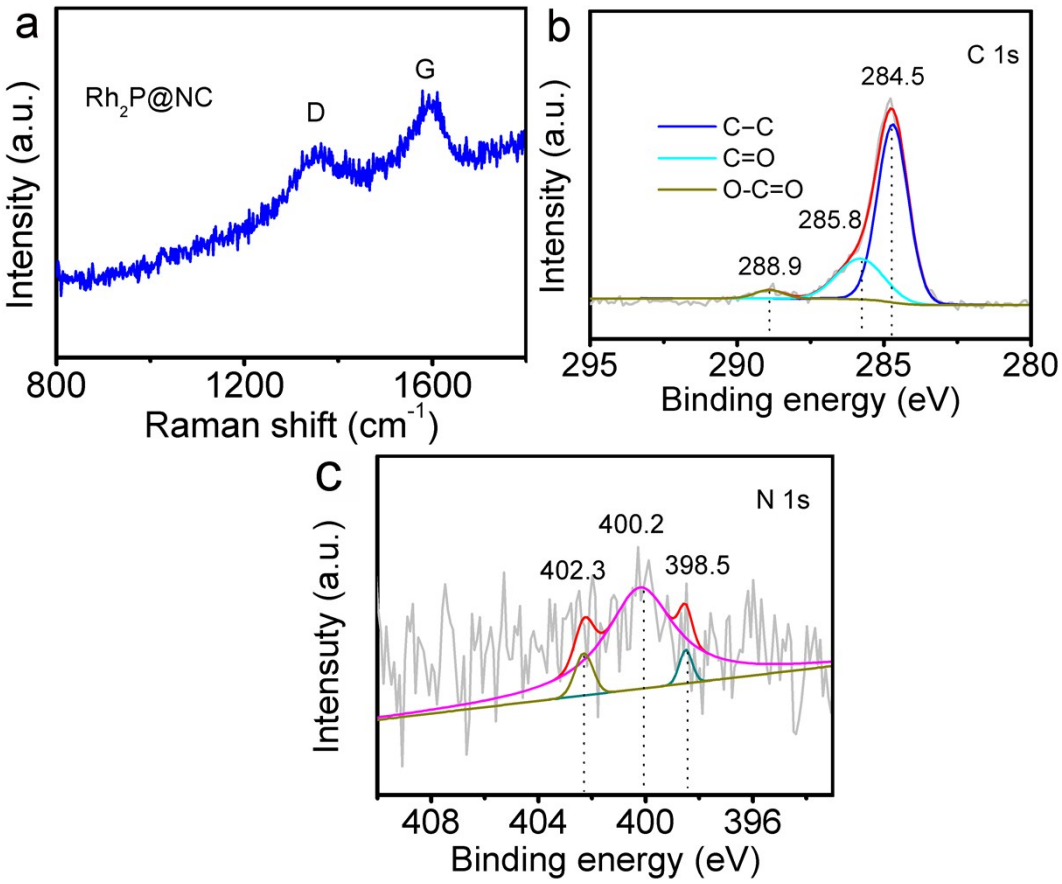

Fig. S3 (a) Raman spectrum of Rh_2P@NC. High-resolution XPS spectrum of (b) C 1s and (c) N 1s.

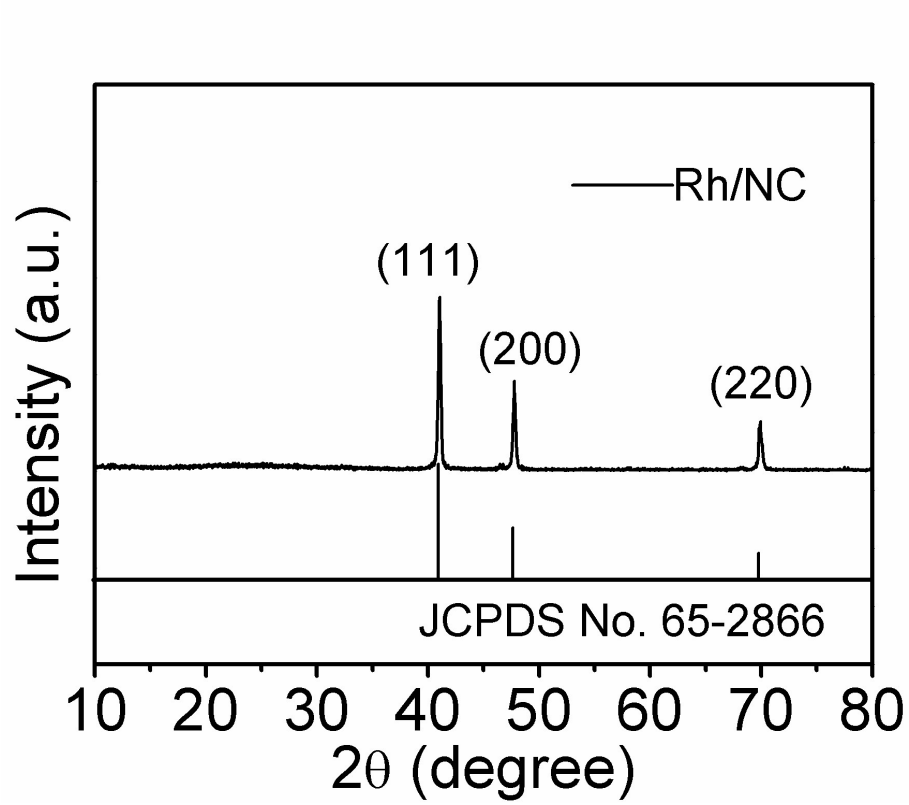

Fig. S4 XRD pattern of Rh/NC.

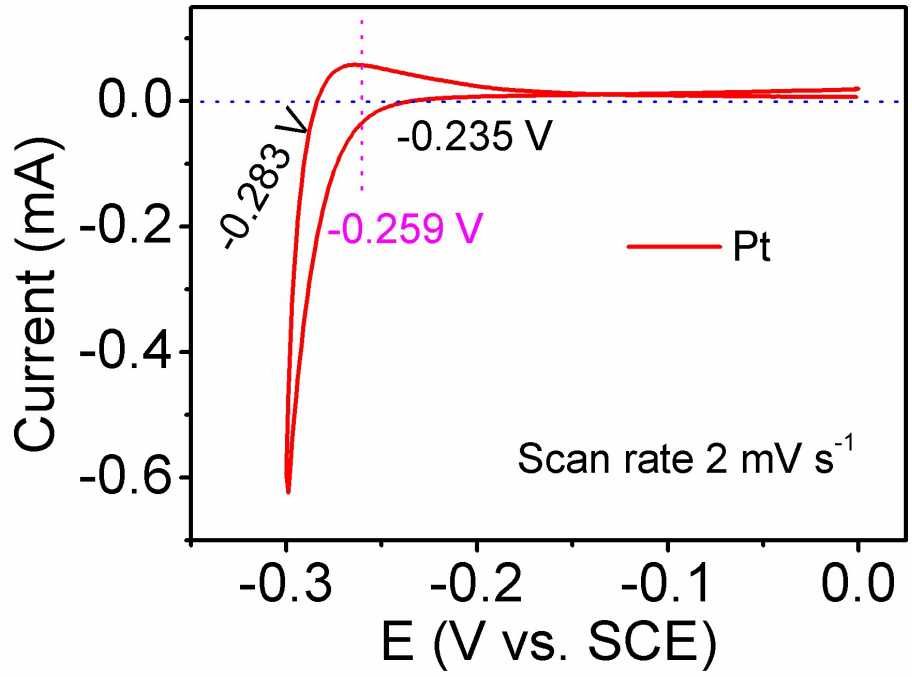

Fig. S5 RHE voltage calibration.

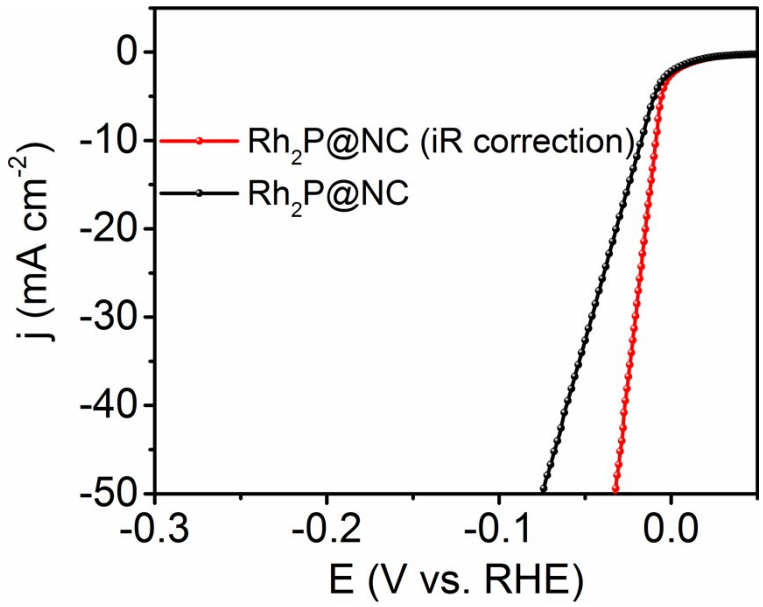

Fig. S6 The polarization curves of the Rh_2P@NC with/without iR correction.

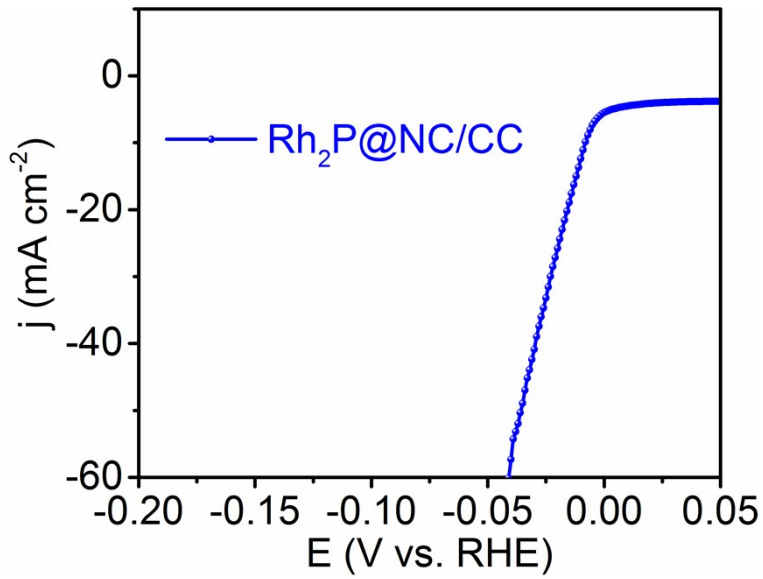

Fig. S7 The polarization curves of the Rh_2P@NC loaded on carbon cloth.

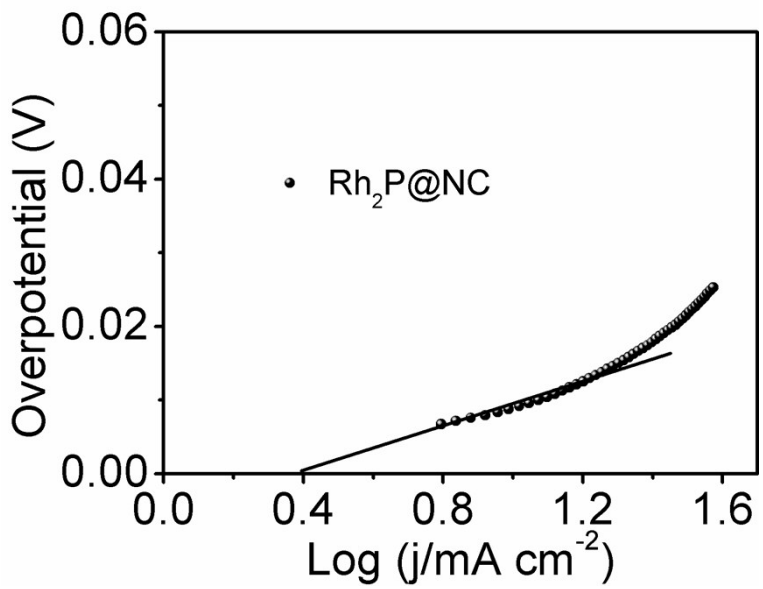

Fig. S8 Calculation of exchange current density of Rh_2P@NC by applying extrapolation method to the Tafel plot.

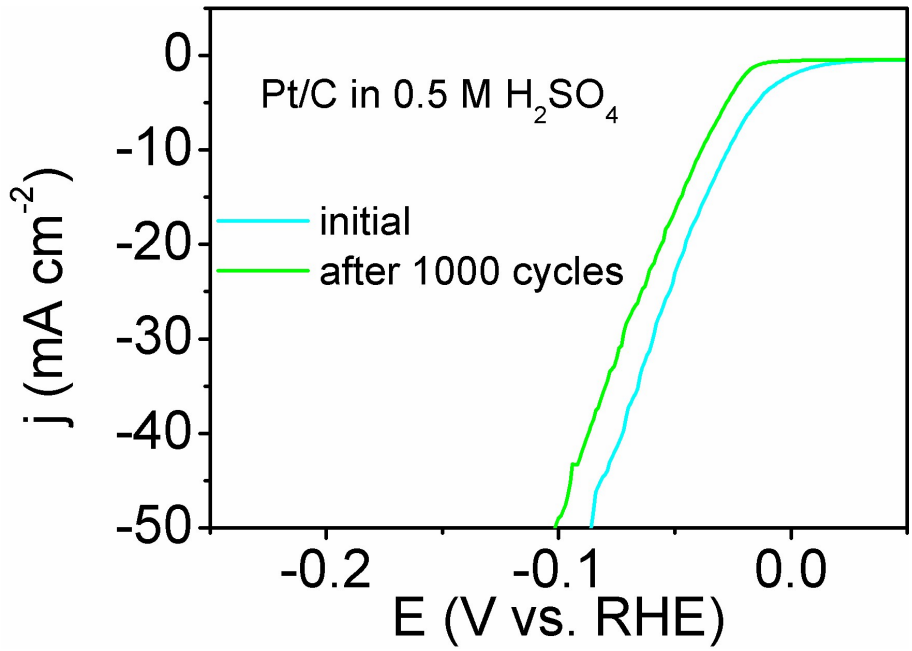

Fig. S9 HER polarization curves were recorded before and after 1000 CV cycles for Pt/C in 0.5 M H_2SO_4 solution.

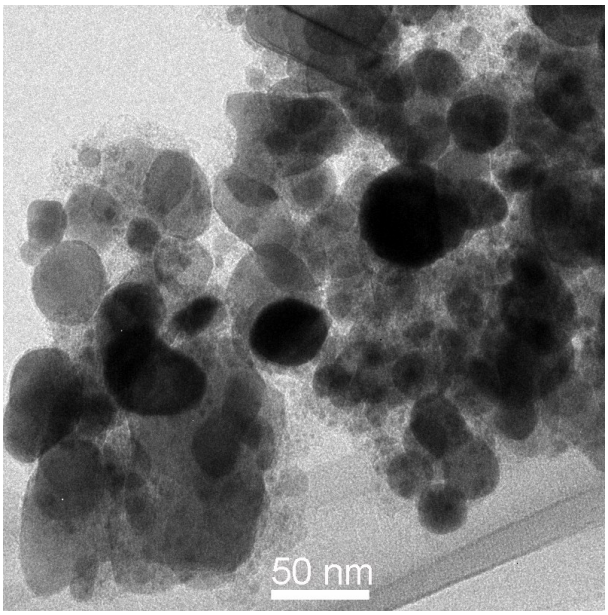

Fig. S10 TEM image of Rh_2P@NC after HER stability test in 0.5 M H_2SO_4.

Table S1 Comparison of HER performance in acid/neutral/alkaline media of Rh_2P@NC with other highly efficient HER electrocatalysts.

Catalysts	Electrolytes/(pH)	Overpotential@j (mV@mA cm^{-2})	Tafel slope (mV dec^{-1})	Catalyst loading (mg cm^{-2})	Ref.
Rh_2P@NC	0.5 M H_2SO_4	9@10	26	0.7	This work
	1.0 M PBS	46@10	37		
	1.0 M KOH	10@10	40		
CoP/CC	0.5 M H_2SO_4	67@10	51	0.92	1
	1.0 M PBS	65@2	93		
	1.0 M KOH	209@10	129		
np-CoP NWs/Ti	0.5 M H_2SO_4	95@20	65	0.8	2
	1.0 M PBS	178@10	125		
	1.0 M KOH	150@20	71		
CoP@BCN	0.5 M H_2SO_4	87@10	46	0.4	3
	1.0 M PBS	122@10	59		
	1.0 M KOH	215@10	52		
WP NAs/CC	0.5 M H_2SO_4	130@10	69	2.0	4
	1.0 M PBS	200@10	125		
	1.0 M KOH	150@10	102		
WP_2 SMPs	0.5 M H_2SO_4	161@10	57	0.5	5
	1.0 M PBS	143@2	92		
	1.0 M KOH	153@10	60		
WP_2 NRs	0.5 M H_2SO_4	347@10	52	-	6
	1.0 M PBS	298@10	79		
	1.0 M KOH	225@10	84		
WP_2 NPs/W	0.5 M H_2SO_4	143@10	66	0.2	7
	1.0 M PBS	201@10	95		
	1.0 M KOH	214@10	92		
WP NPs@NC	0.5 M H_2SO_4	102@10	58	2.0	8

	1.0 M PBS	196@10			
	1.0 M KOH	150@10			
MoP_2 NS/CC	0.5 M H_2SO_4	58@10	63.6	0.8	9
	1.0 M PBS	67@10	98.3		
	1.0 M KOH	85@10	70.0		
MoP NA/CC	0.5 M H_2SO_4	124@10	58	2.5	10
	1.0 M PBS	187@10	94		
	1.0 M KOH	80@10	83		
MoP_2 NPs/Mo	0.5 M H_2SO_4	143@10	57	-	11
	1.0 M PBS	211@10	81		
	1.0 M KOH	194@10	80		
MoP NPs@NC	0.5 M H_2SO_4	115@10	65	2.0	12
	1.0 M PBS	136@10	71		
	1.0 M KOH	80@10	59		
FeP NPs@NPC	0.5 M H_2SO_4	130@10	67	1.4	13
	1.0 M PBS	386@10	136		
	1.0 M KOH	214@10	82		
Mn-CoP/Ti	0.5 M H_2SO_4	49@10	55	5.61	14
	1.0 M PBS	86@10	82		
	1.0 M KOH	76@10	52		
$NiCo_2P_x$/CF	0.5 M H_2SO_4	104@10	59.6	5.9	15
	1.0 M PBS	63@10	63.3		
	1.0 M KOH	58@10	34.3		
np-$(Co_{052}Fe_{0.48})_2P$	0.5 M H_2SO_4	64@10	45	2.5	16
	1.0 M KOH	79@10	40		
Ni_2P/Ti	0.5 M H_2SO_4	130@20	46	1.0	17
Ni_2P	0.5 M H_2SO_4	140@20	66	0.38	18
	1.0 M KOH	250@20	102		
NiP_2 NS/CC	0.5 M H_2SO_4	75@10	51	4.3	19
	1.0 M KOH	102@10	65		

CoP/CNT	0.5 M H_2SO_4	122@10	54	0.285	20
CoP/Ti	0.5 M H_2SO_4	85@20	50	2.0	21
Co-P/Cu foil	1.0 M NaOH	94@10	42	-	22
FeP	0.5 M H_2SO_4	50@10	37	1.0	23
MoP	0.5 M H_2SO_4	180@30	54	0.86	24
Mo_2C@NC	0.5 M H_2SO_4	124@10	-	0.28	25
	0.5 M PBS	156@10	-	-	
	1.0 M KOH	60@10	-		
15-h-CoS_2	0.5 M H_2SO_4	200@12.37	72	-	26
	1.0 M PBS	~240@10	129		
	1.0 M KOH	244@10	133		
Co-NCNT/CC	0.5 M H_2SO_4	78@10	74	3.4	27
	1.0 M PBS	170@10	97		
	1.0 M KOH	180@10	193		
CoNC/GD	0.5 M H_2SO_4	340@10	138	-	28
	1.0 M PBS	368@10	207		
	1.0 M KOH	284@10	115		
WN NA/CC	0.5 M H_2SO_4	198@10	62	2.5	29
	1.0 M PBS	302@10	182		
	1.0 M KOH	285@10	170		
WON@NC	0.5 M H_2SO_4	106@10	65	7.7	30
NAs/CC	1.0 M PBS	152@10	142		
	1.0 M KOH	130@10	128		
Mo_2C	0.5 M H_2SO_4	136@10	68.4	1.0	31
QD/NGCL	1.0 M PBS	136@10	81.9		
	1.0 M KOH	111@10	57.8		
P-W_2C@NC	0.5 M H_2SO_4	89@10	53	3.5	32
	0.1 M PBS	185@10	-		
	1.0 M KOH	63@10			
1D-RuO_2-CN_x	0.5 M H_2SO_4	93@10	40	~0.17	33

	0.1 M PBS	356@10	135		
	0.5 M KOH	95@10	70		
Co-Ni-B	0.1 M $HClO_4$	209@10	-	2.1	34
	0.5 M KPi	170@10	51		
	1.0 M NaOH	133@10	-		
$Zn_{0.3}Co_{2.7}S_4$	0.5 M H_2SO_4	80@10	47.5	0.285	35
	0.1 M PBS	90@10	-		
	1.0 M KOH	85@10			
CNF@CoS_2	0.5 M H_2SO_4	110@10	66.8	6.6	36
	1.0 M PBS	360@10	163.7		
	1.0 M KOH	207@10	113.3		
Ni-C-N NSs	0.5 M H_2SO_4	60.9@10	32	0.2	37
	1.0 M PBS	92.1@10	-		
	1.0 M KOH	30.8@10	-		
Co-C-N	0.5 M H_2SO_4	138@10	55	-	38
	1.0 M PBS	276@10	107		
	1.0 M KOH	178@10	102		
Co-NRCNTs	0.5 M H_2SO_4	260@10	80	0.28	39
	1.0 M PBS	540@10	-		
	1.0 M KOH	370@10	-		
Co-Mo-S_x	0.1 M $HClO_4$	~250@5	-	0.05	40
	0.1 M KOH	~201@5	-		
NiAu/Au	0.5 M H_2SO_4	~50@10	36	-	41
Rh_2P/C	0.5 M H_2SO_4	5.4@5	-	0.0037	42
	0.1 M KOH	30.8@5			
Rh_2S_3	0.5 M H_2SO_4	122@10	44	0.92	43
Ru/C_3N_4/C	0.5 M H_2SO_4	~75@10	-	-	44
	0.1 M KOH	79@10			
C_3N_4@NG	0.5 M H_2SO_4	240@10	51.5	0.1	45

2. **Theoretical calculation**

2.1 DFT Computational Methods. The Plane-wave Density Functional Theory (DFT) calculations were conducted using the CASTEP module (an Ab Initio Total Energy Program) of Materials Studio 8.0 (Code version: 6546), with the hydrogen binding energy calculated from different active sites.[46] The generalized gradient approximation (GGA) method with a Perdew-Burke-Ernzerhof (PBE) functional was used to treat the electron exchange correlation (EEC) interaction. The band energy and Fermi energy convergence tolerance were set at 1.0 $\times 10^{-5}$ and 2.7 $\times 10^{-5}$ eV, respectively. The DOS kpoint separation was set at 0.05 $Å^{-1}$. A Monkhorst–Pack grid k-points of 3×1×1 and a plane wave basis set cut-off energy of 300 eV were used for the Brillouin zone integration. The structures were optimized for force and energy convergence set at 2.0×10^{-5} eV and 0.05 eV $Å^{-1}$, respectively. The self-consistence field (SCF) was 2.0×10^{-6} eV/atom. To consider the influence of van der Waals interaction, the semi-empirical DFT-D force-field approach was applied.[47,48] The Gibb's free energies for hydrogen absorption ΔG_{H*} were calculated from the given equation:

$$\Delta G_{H*} = \Delta E_{H*} + \Delta ZPE - T\Delta S$$

Where the symbols represent the binding energy (ΔE), the change in zero-point energy (ΔE_{ZPE}), Temperature (T), and the entropy change (ΔS) of the system, respectively. The TΔS and ΔZPE are obtained as previously reported by Norskov et al. [4] Thus, we adopted the approximation that the vibrational entropy of hydrogen in the adsorbed state is negligible, in which case $\Delta S_H \approx S_{H*} - 1/2(S_{H2}) \approx -1/2(S_{H2})$, where S_{H2} is the entropy of H_2(g) at standard conditions, and $TS(_{H2})$ is ~0.41 eV for H_2 at 300 K and 1 atm.[49]

2.2 Theoretical models. We build the correlative theoretical models to simulate the C, NC, Rh/NC and Rh_2P@NC. The pure carbon layer is simulated by the single-layer

undoped carbon (C) or N-doped carbon (NC) as shown in **Fig. S8a** and **S8b**, respectively. The composite Rh_2P@NC model is constructed by covering the respective NC layer on the (200) facet of the Rh_2P slab (**Fig. S8d**). To minimize the effects of lattice mismatch between the Rh_2P and NC, we considered an interface periodicity of 2×2 and 2×2 supercells for the Rh_2P and NC phases of Rh_2P@NC, respectively. The lattice parameters for all models are presented in **Table S2**.

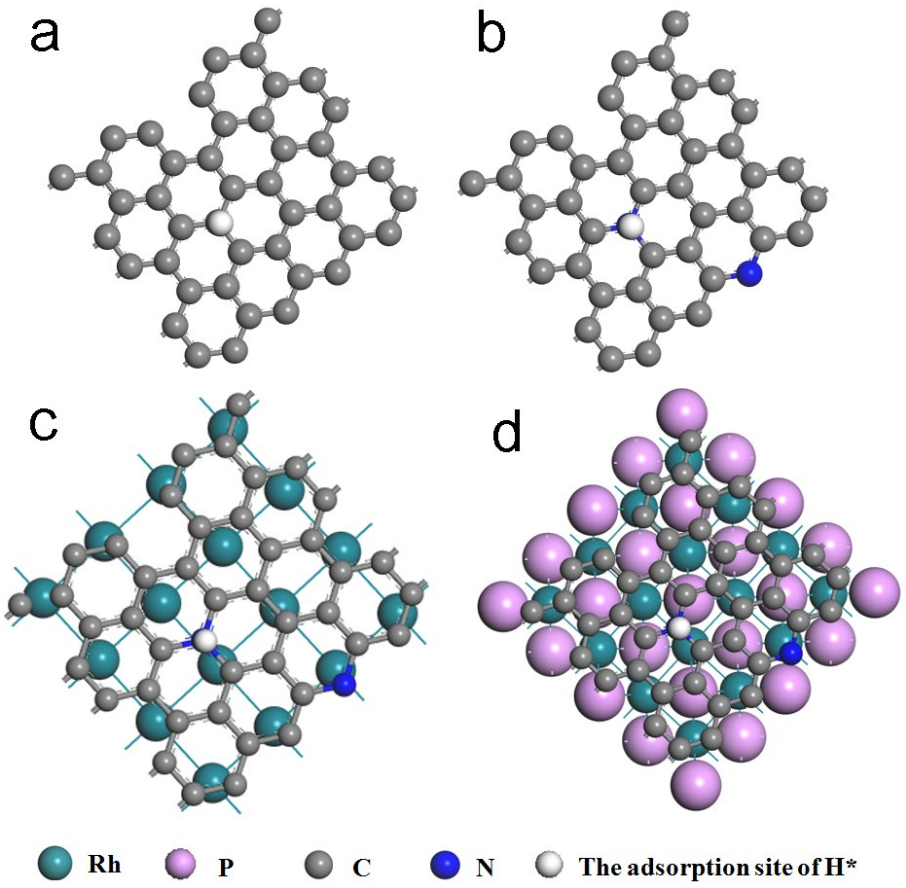

Fig. S8. The theoretical models used in DFT calculations and the adopted adsorption sites of H* on the surface of these models: (a) C, (b) NC, (c) Rh/NC and (d) Rh_2P@NC.

Table S2 The lattice parameters (Å) of the supercells for all the systems.

Models	a	b	c
C	9.840	9.840	15.000
NC	9.841	9.841	15.000
Rh/NC	11.127	11.127	17.782
Rh_2P@NC	11.127	11.127	17.782

References

1 J. Tian, Q. Liu, A. M. Asiri and X. Sun, *J. Am. Chem. Soc.,* 2014, **136**, 7587–7590.

2 S. Gu, H. Du, A. M. Asiri, X. Sun and C. Li, *Phys. Chem. Chem. Phys*., 2014, **16**, 16909–16913.

3 H. Tabassum, W. Guo, W. Meng, A. Mahmood, R. Zhao, Q. Wang and R. Zou, *Adv. Energy Mater.,* DOI: 10.1002/aenm.201601671.

4 Z. Pu, Q. Liu, A. M. Asiri and X. Sun, *ACS Appl. Mater. Interfaces,* 2014, **6**, 21874–21879.

5 Z. Xing, Q. Liu, A. M. Asiri and X. Sun, *ACS Catal.,* 2015, **5** 145–149.

6 H. Du, S. Gu, R. Liu and C. Li, *J. Power Sources,* 2015, **278**, 540–545.

7 Z. Pu, I. S. Amiinu and S. Mu, *Energy Technol.,* 2016, **4**, 1030–1034.

8 Z. Pu, X. Ya, I. S. Amiinu, Z. Tu, X. Liu, W. Li and S. Mu, *J. Mater. Chem. A,* 2016, **4**, 15327–15332.

9 W. Zhu, C. Tang, D. Liu, J. Wang, A. M. Asiri and X. Sun, *J. Mater. Chem. A,* 2016, 4, 7169–7173.

10 Z. Pu, S. Wei, Z. Chen and S. Mu, *Appl. Catal. B: Environ.,* 2016, **196***,* 193–198.

11 Z. Pu, I. S. Amiinu, M. Wang, Y. Yang and S. Mu, *Nanoscale,* 2016, **8**, 8500–8504.

12 Z. Pu, I. S. Amiinu, X. Liu, M. Wang and S. Mu, *Nanoscale,* 2016, **8**, 17256–17261.

13 Z. Pu, Y. Xue, I. S. Amiinu, C. Zhang, M. Wang, Z. Kou and S. Mu, *Nanoscale,* 2017, **9**, 3555–3560.

14 T. Liu, X. Ma, D. Liu, S. Hao, G. Du, Y. Ma, A. M. Asiri, X. Sun, L. Chen, *ACS Catal.* **2017**, *7*, 98–102.

15 R. Zhang, X. Wang, S. Yu, T. Wen, X. Zhu, F. Yang, X. Sun, X. Wang and W. Hu, *Adv. Mater.,* 2017, 1605502.

16 Y. Tan, H. Wang, P. Liu, Y. Shen, C. Cheng, A. Hirata, T. Fujita, Z. Tang and M. Chen, *Energy Environ. Sci.,* 2016, **9**, 2257–2261.

17 E. J. Popczun, J. R. McKone, C. G. Read, A. J. Biacchi, A. M. Wiltrout, N. S. Lewis and R. E. Schaak, *J. Am. Chem. Soc.,* 2013, **135**, 9267–9270.

18 L. Feng, H. Vrubel, M. Bensimon and X. Hu, *Phys. Chem. Chem. Phys.,* 2014, **16**, 5917–5921.

19 P. Jiang, Q. Liu and X. Sun, *Nanoscale,* 2014, **6**, 13440–13445.

20 Q. Liu, J. Tian, W. Cui, P. Jiang, N. Cheng, A. M. Asiri and X. Sun, *Angew. Chem., Int. Ed.,* 2014, **53**, 6710–6714.

21 E. J. Popczun, C. G. Read, C. W. Roske, N. S. Lewis and R. E. Schaak, *Angew. Chem. Int. Ed.,* 2014, **126**, 5531–5534.

22 N. Jiang, B. You, M. Sheng and Y. Sun, *Angew. Chem., Int. Ed.,* 2015, **54**, 6251–6254.

23 F. Juan, J. Callejas, M. McEnaney, C. G. Read, J. C. Crompton, A. J. Biacchi, E. J. Popczun, T. R. Gordon, N. S. Lewis and R. E. Schaak, *ACS Nano,* 2014, **8**,

11101–11107.
24 P. Xiao, M. A. Sk, L. Thia, X. Ge, R. J. Lim, J. Y. Wang, K. H. Li and X. Wang, *Energy Environ. Sci.,* 2014, **7**, 2624–2629.
25 X. Zou, X. Huang, A. Goswami, R. Silva, B. R. Sathe, E. Mikmekova and T. Asefa, *Angew. Chem., Int. Ed.,* 2014, **126**, 4372–4376.
26 H. Zhang, Y. Li, G. Zhang, P. Wan, T. Xu, X. Wu and X. Sun, *Electrochimi. Acta,* 2014, **148**, 170–174.
27 Z. Xing, Q. Liu, W. Xing, A. M. Asiri and X. Sun, *ChemSusChem,* 2015, **8**, 1850–1855.
28 Y. Xue, J. Li, Z. Xue, Y. Li, H. Liu, D. Li, W. Yang and Y. Li, *ACS Appl. Mater. Interfaces,* 2016, **8**, 31083−31091.
29 J. Shi, Z. Pu, Q. Liu, A. M. Asiri, J. Hu and X. Sun, *Electrochimi. Acta,* 2015, **154**, 345–351.
30 Q. Li, W. Cui, J. Tian, Z. Xing, Q. Liu, W. Xing, A. M. Asiri and X. Sun, *ChemSusChem,* 2015, **8**, 2487–2491.
31 Z. Pu, M. Wang, Z. Kou, I. S. Amiinu and S. Mu, *Chem. Commun.,* 2016, **52**, 12753–12756.
32 G. Yan, C. Wu, H. Tan, X. Feng, L. Yan, H. Zang and Y. Li, *J. Mater. Chem. A,* 2017, **5**, 765–772.
33 T. Bhowmik, M. Kundu and S. Barman, *ACS Appl. Mater. Interfaces,* 2016, **8**, 28678−28688.
34 S. Gupta, N. Patela, R. Fernandes, R. Kadrekar, A. Dashora, A. K. Yadav, D. Bhattacharyya, S. N. Jha, A. Miotello and D. C. Kothari, *Appl. Catal. B: Environ*., 2016, **192**, 126–133.
35 Z. Huang, J. Song, K. Li, M. Tahir, Y. Wang, L. Pan, L. Wang, X. Zhang and J. Zou, *J. Am. Chem. Soc.,* 2016, **138**, 1359–1365.
36 H. Gu, Y. Huang, L. Zuo, W. Fan and T. Liu, *Inorg. Chem. Front.,* 2016, **3**, 1280–1288.
37 J. Yin, Q. Fan, Y. Li, F. Cheng, P. Zhou, P. Xi and S. Sun, *J. Am. Chem. Soc.,* 2016, **138**, 14546–14549.
38 S. Wang, X. Hao, Z. Jiang, X. Sun, D. Xu, J. Wang, H. Zhong, F. Meng and X. Zhang, *J. Am. Chem. Soc.,* 2015, **137**, 15070–15073.
39 X. Zou, X. Huang, A. Goswami, R. Silva, B. R. Sathe, E. Mikmekova and T. Asefa, *Angew. Chem., Int. Ed.,* 2014, **126**, 4461-4465.
40 J. S. Jirkovský, C. D. Malliakas, P. P. Lopes, N. Danilovic, S. S. Kota, K. C. Chang, B. Genorio, D. Strmcnik, V. R. Stamenkovic, M. G. Kanatzidis and N. M. Markovic, *Nat. Mater.,* 2016, **15**, 197–203.
41 H. Lv, Z. Xi, Z. Chen, S. Guo, Y. Yu, W. Zhu, Q. Li, X. Zhang, M. Pan, G. Lu, S. Mu and S. Sun, *J. Am. Chem. Soc.,* 2015, **137**, 5859–5862.
42 H. Duan, D. Li, Y. Tang, Y. He, S. Ji, R. Wang, H. Lv, P. P. Lopes, A. P. Paulikas, H. Li, S. X. Mao, C. Wang, N. M. Markovic, J. Li, V. R. Stamenkovic and Y. Li, *J. Am. Chem. Soc.,* 2017, **139**, 5494–5502.
43 D.Yoon, B. Seo, J. Lee, K. S. Nam, B. Kim, S. Park, H. Baik, S. H. Joo and K. Lee, *Energy Environ. Sci.,* 2016, **9**, 850–856.

44 Y. Zheng, Y. Jiao, Y. Zhu, L. H. Li, Y. Han, Y. Chen, M. Jaroniec and S. Qiao, *J. Am. Chem. Soc.,* 2016, **138**, 16174–16181.
45 Y. Zheng, Y. Jiao, Y. Zhu, L. H. Li, Y. Han, Y. Chen, A. Du, M. Jaroniec and S. Z. Qiao, *Nat. Commnu.,* 2014, **5**, 3783.
46 M. Segall, P. J. Lindan, M. Probert, C.Pickard, P. Hasnip, S.Clark and M. Payne. *J. Phys. Condens. Matter*., 2002, **14**, 2717.
47 G. Kresse and D. Joubert, *Phys. Rev. B,* 1999, **59**, 1758–1775.
48 S. J. Grimme, *Comput. Chem.,* 2006, **27**, 1787–1799.
49 K. Nørskov, T. Bligaard, A. Logadottir, J. R. Kitchin, J. G. Chen, S. Pandelov and U. Stimming. *J. Electrochem. Soc.,* 2005, **152**, J23.